Bulletin of the Seismological Society of America, Vol. 84, No. 4, pp. 963–973, August 1994

Some Observations of Landslides Triggered by the 29 April 1991 Racha Earthquake, Republic of Georgia

by R. W. Jibson, C. S. Prentice, B. A. Borissoff, E. A. Rogozhin, and C. J. Langer

Abstract On 29 April 1991 an M_S 7.0 earthquake occurred in the Racha region of the Great Caucasus Mountains in north-central Republic of Georgia. The earthquake occurred on a thrust fault striking roughly east–west and dipping about 20° to 45° northward; focal depth was 17 ± 2 km. We observed no surface fault rupture, but the earthquake caused extensive structural damage to the many unreinforced stone buildings in the area, and at least 114 people were killed. Many landslides were triggered in a 2500-km^2 epicentral area, and they caused much of the structural damage and at least half the fatalities. We observed the following six types of landslides (in order of decreasing abundance): rock falls, debris slides, slumps, earth slides, rock block slides, and rock avalanches. The types of landslides triggered by the earthquake are controlled primarily by lithology and geologic structure. Enigmatic landslide processes associated with this earthquake include (1) delays of several days between earthquake shaking and significant landslide movement, probably caused by changes in groundwater conditions; (2) small co-seismic displacement of landslides active at the time of the earthquake, a possible result of viscoplastic damping of the seismic shaking; and (3) somewhat unusual failure geometries related to local topography and geologic structure.

Introduction

On 29 April 1991 an M_S 7.0 earthquake occurred in the Racha region of the Great Caucasus Mountains in north-central Republic of Georgia (Fig. 1). This is the largest earthquake in the nearly 200-yr historical record available for the area (Riznichenko and Dzhibladze, 1974; Kondorskaya and Shebalin, 1982; Gorshkov, 1984). The mainshock and several of its aftershocks caused at least 114 fatalities, injured about 1000 people, left more than 67,000 homeless, and caused widespread damage. Strong ground shaking reached a maximum Modified Mercalli intensity of VIII. By far the most significant geologic effect of the earthquake was abundant co-seismic and postseismic landsliding that caused extensive damage and at least half of the fatalities.

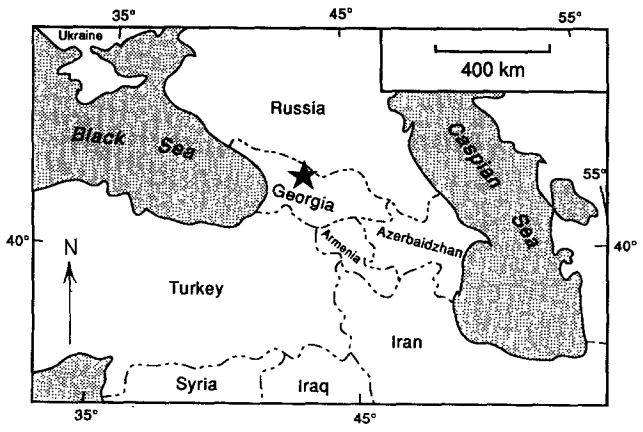

Figure 1. Map showing epicenter (star) of 29 April 1991 Racha earthquake in the Republic of Georgia.

The Racha earthquake occurred on the southern flank of the western Great Caucasus Mountains in a very mobile area within the active collision zone between the Arabian and Eurasian plates (Fig. 2). This region is characterized by southward-directed thrusting of folded Paleozoic, Mesozoic, and Paleogene volcanic and sedimentary rocks over Neogene and Quaternary sediments of the Rioni Basin (Milanovsky and Khain, 1963; Zonenshain and Le Pichon, 1986; Philip *et al.*, 1989), a process that continues today and has created an active zone of thrusting and strike-slip faulting. However, no earthquakes of $M \geqq 7$, other than the 1991 event, have occurred in the Caucasus since A.D. 1800 (Gorshkov, 1984; Philip *et al.*, 1989), which suggests a low rate of seismicity, considering that convergence rates as great as 28 mm/yr between the Arabia and Eurasia plates are

predicted by plate-motion models (Jackson and McKenzie, 1984, 1988; Philip *et al.*, 1989; DeMets *et al.*, 1990). Thus, much of the deformation across the Caucasus is thought to be aseismic (Jackson, 1992).

The mainshock (m_b 6.2, M_S 7.0, **M** 7.1) of 29 April 1991 was located at 42.453° N, 43.673° E at a focal depth of 17 ± 2 km; the moment was 8×10^{19} Nm (U.S. Geological Survey, 1991). The focal-plane solution most consistent with the regional tectonics shows pure thrust on a surface striking roughly east–west and dipping northward 20° to 45°. Borissoff and Rogozhin (1992) proposed an alternative focal mechanism involving underthrusting on a series of en-echelon faults that strike N60°W and dip about 15° NE; this model requires a shallower focal depth of 6 to 14 km. Figure 3 shows the mainshock epicenter and the area of aftershocks recorded from 3 May to 6 July 1991 by 45 portable seismographs. The two largest aftershocks were an M_S 6.0 about 9 hr after the mainshock and an M_S 6.5 on 15 June.

Borissoff and Rogozhin (1992) conducted a broad-scale geological field investigation of the epicentral region from 2 May through 20 August 1991; Jibson, Prentice, and Langer joined this investigation from 10 to 19 May 1991 to document earthquake-triggered ground failure (Jibson and Prentice, 1991) and record aftershocks. Our investigation of ground failure was limited to a fairly brief reconnaissance of the epicentral area, and we lack quantitative geologic, geotechnical, and hydrologic data that would be needed for detailed analysis of the documented features. Our investigation was further hampered by lack of large-scale base maps of the epicentral area; therefore, we could locate specific observations and photographs only approximately by referring to place names shown on the epicentral map (Fig. 3), which was derived from a U.S. Defense Mapping Agency, 1:500,000-scale base.

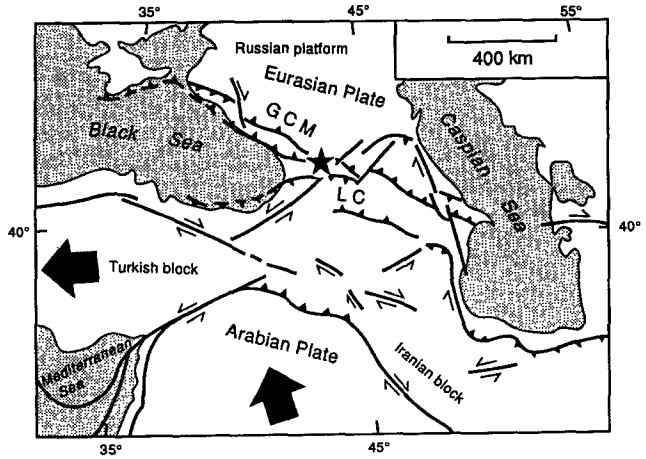

Figure 2. Map showing regional tectonic setting (modified from Philip *et al.*, 1989 and Jackson, 1992). Heavy lines are major faults; barbs on upper plates of thrusts, small arrows indicate relative strike-slip motion. Star indicates epicenter of 29 April 1991 Racha earthquake; GCM is Great Caucasus Mountains, LC is Lesser Caucasus. Large arrows show plate motions relative to a stable Eurasian Plate (Jackson and McKenzie, 1984; DeMets *et al.*, 1990).

We observed no surface fault rupture associated with this earthquake, which, in light of the high magnitude and moderately shallow depth, is unusual but not unprecedented. We likewise saw no evidence that the mainshock induced liquefaction of coarse-grained sediment, although the 15 June aftershock (M_S 6.5) did trigger minor liquefaction on a flood plain near Dzhava (Fig. 3). We saw significant shaking-induced structural damage, which was most severe in remote villages at higher elevations in the Great Caucasus Mountains. These villages consist primarily of older, unreinforced structures having uncemented or poorly cemented stone walls, many of which collapsed or were severely damaged during the earthquake. Larger towns in river valleys had greater proportions of newer, wood-frame and reinforced-masonry structures that generally sustained only slight or moderate damage. The only modern, multi-story building in the epicentral region in which we observed severe damage was a five-story, unreinforced concrete apartment building in Ambrolauri (Fig. 3), whose center section collapsed during an M_S 5.3 aftershock on 3 May 1991. At greater distances, buildings collapsed as far away as Chiatura (Fig. 3).

Landslides were by far the most significant geologic effect of this earthquake. In the sections that follow, we briefly describe the distribution and types of landslides triggered by the earthquake in the epicentral area, and compare our observations with characteristics of ground failure determined from analysis of worldwide earthquakes. We then focus on some enigmatic characteristics of this landsliding, such as delays of 2 to 3 days between the earthquake and triggered movement of existing landslides, small co-seismic displacement of active landslides, and unusual failure geometries. Such phenomena have seldom been documented and challenge some current ideas about the seismic behavior of landslides.

Distribution and Types of Landslides Triggered by the Earthquake

Landslide Distribution

The earthquake triggered and reactivated many landslides throughout the epicentral area, which caused a large proportion of the damage. We documented landslides over an area about 90 by 30 km having a total area of ~2500 km^2 (Fig. 3). The farthest limits of landsliding are based on ground and aerial reconnaissance observations of rock falls, the type of landslide that worldwide observations indicate typically occur at the greatest epicentral distances (Keefer, 1984). The northern, southern, and

western limits of landsliding are fairly well established and coincide roughly with the area of the aftershock zone; the eastern limit is somewhat less certain because of restricted access. The northwestern landslide limit also coincides with the Rioni–Kazbek fault, and the northeastern limit, to a lesser degree, parallels the Utsera fault (Fig. 3). Borissoff and Rogozhin (1992) suggested that these faults define the limit of the meizoseismal area because earthquake effects were observed to decrease abruptly across these structures. Because the epicenter of the mainshock is in the eastern part of the study area, and the aftershocks extend farther to the southeast, the total area affected by landslides could extend as far to the east and southeast of the epicenter as the western boundary extends to the west. Thus, the total area affected by landslides could be perhaps 25% larger (~3000 km^2) than the area we documented. In other earthquakes of this magnitude worldwide, the maximum areas affected by landslides are about 24,000 km^2 (Keefer, 1984), and the average areas affected are about 6000 km^2 (Keefer and Wilson, 1989). Thus, the area affected by landslides in the Racha earthquake is an order of magnitude smaller than the maximum area and about half as large as the average area that might be expected. Within the broad area affected by landslides is a much smaller area (about 400 km^2) of more concentrated landslide activity (Fig. 3). In addition to rock falls, this smaller area contains many large, deep-seated landslides triggered by the earthquake.

Landslide Types

In the epicentral region, rapid tectonic uplift, active fluvial incision, and abundant precipitation combine to produce steep slopes, deep weathering of surficial materials, and, consequently, widespread slope instability. Except for rock avalanches, every type of landslide triggered by the earthquake also was active in the area before the earthquake. We saw many landslides that initially appeared related to the earthquake; however, closer inspection indicated that they had moved in response to spring rains within a few weeks before the earthquake. The earthquake triggered six broad types of landslides in the epicentral area; in decreasing order of abundance they include rock falls, debris slides, earth slides, slumps, rock block slides, and rock avalanches (Fig. 4, classification of Varnes, 1978). In general, landslide types and distribution were strongly controlled by lithology and geologic structure.

Rock Falls. The earthquake triggered hundreds of rock falls from near-vertical escarpments in Mesozoic limestone and on steep slopes along road and stream cuts in Jurassic volcanic rocks. The most notable example is a nearly vertical, 100-m-high limestone scarp extending

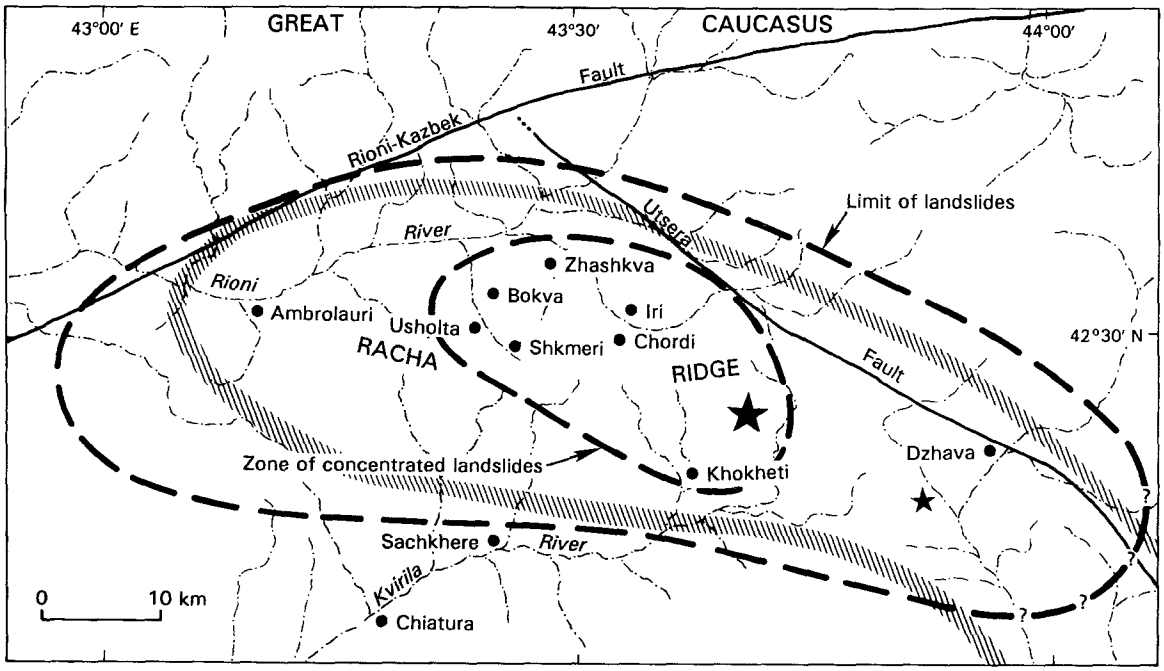

Figure 3. Map of epicentral area. Large star is mainshock epicenter; small star is M_S 6.5 aftershock of 15 June; hachured boundary outlines aftershock zone; outer heavy dashed line is limit of observed earthquake-triggered landslides, queried where uncertain; inner heavy dashed line outlines zone of concentrated landslide activity; solid lines are major faults; dash-dot lines are principal streams and rivers.

TYPE OF MOVEMENT			TYPE OF MATERIAL		
			BEDROCK	ENGINEERING SOILS	
				Predominantly coarse	Predominantly fine
FALLS			Rock fall	Debris fall	Earth fall
TOPPLES			Rock topple	Debris topple	Earth topple
SLIDES	ROTATIONAL	FEW UNITS	Rock slump	Debris slump	Earth slump
	TRANSLATIONAL	FEW UNITS	Rock block slide	Debris block slide	Earth block slide
		MANY UNITS	Rock slide	Debris slide	Earth slide
LATERAL SPREADS			Rock spread	Debris spread	Earth spread
FLOWS			Rock flow (deep creep)	Debris flow (soil creep)	Earth flow
COMPLEX			Combination of two or more principal types of movement		

Figure 4. Table summarizing landslide classification by type of material and type of movement (from Varnes, 1978, p. 11).

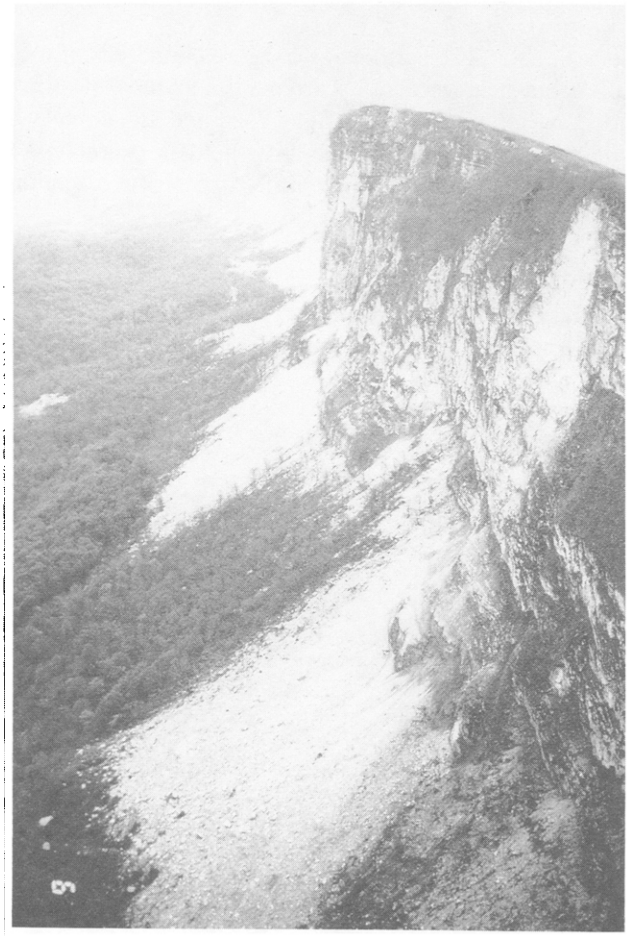

Figure 5. Limestone escarpment along Racha Ridge between Bokva and Usholta (see Fig. 3) that produced many large rock falls. Note fresh rock-fall deposit at base of scarp and fresh rock-fall scar at upper right. Scarp is more than 100-m high.

along Racha Ridge between Bokva and Usholta (Fig. 3), which produced several large rock falls (Fig. 5). The scarp is on the north flank of an anticline, and the limestone dips out of the escarpment as steeply as 40°. Joint orientation appears random, and spacing varies between 0.3 and 7 m; rock-fall source areas commonly are defined by intersecting joint surfaces. Some of these joints opened several centimeters as a result of the earthquake, which may have contributed to slope instability. The rock-fall deposits abut the scarp and form an almost continuous apron as steep as 55° along the base of the scarp. Individual rocks in the fresh deposits range from a few centimeters to 7 m across. Many of the larger blocks left prominent impact craters a few meters apart, which indicates very rapid movement.

Belousov and Chicagov (1993) reported several instances of boulders bouncing and rolling down slopes on a ridge near the epicenter after being thrown vertically into the air, which indicates local vertical accelerations exceeding 1 *g*. They attributed these high accelerations to close proximity to the seismic source and to a vibrating membrane effect of the limestone slab that caps the ridge.

Debris Slides. The earthquake also triggered dozens of debris slides, which typically are parabolic in plan view, on slopes steeper than about 35° along road and stream cuts (Fig. 6). Debris slides generally were confined to weathered volcanic bedrock and overlying colluvium or weakly cemented alluvium of stream terraces. Debris slides in the area range from a few meters to several tens of meters across and hundreds of meters long. Depths generally are about 0.5 to 4 m, but some debris slides are 15 m deep or more.

Slumps. Dozens of slumps formed on steep cut banks of streams and rivers as well as on roads. Most of these

Figure 6. Typical debris slide in unconsolidated colluvium and residuum; slide is about 50-m long by 20-m wide.

slumps were fairly small (less than 10 m wide), but many in the eastern part of the epicentral area were large enough to block streams and temporarily impound ponds and lakes. Slumps were particularly abundant in the area around the town of Iri (Fig. 3), which itself is built on the head of a large, ancient slump in deeply weathered Jurassic volcanic rocks. During the earthquake, extensive ground cracks formed in Iri near the base of the ancient headwall scarp and high on the previously stable slope above the town. The cracks along the main scarp had about 20 cm of total offset and extend through several buildings; the ground cracks above town were reported by eyewitnesses to be "too large to step across." The slopes below town are precipitously steep owing to active fluvial incision, and they contain several shallow slides and slumps triggered by this incision.

Earth Slides. The earthquake triggered several earth slides in the Oligocene–Miocene Maikop Formation, an intensely deformed claystone that weathers to form a weak, plastic soil that can absorb a large volume of water. Most areas underlain by this claystone have experienced recent landslide movement related to seasonal rainfall. These landslides are complex and locally have characteristics of both earth slides and slow earth flows, and parts of some main scarps and oversteepened toes have slumped or toppled. The largest of the earth slides, described subsequently, have volumes of tens of millions of cubic meters.

Rock Block Slides. Several earthquake-triggered rock block slides formed on bedding-plane surfaces of dip slopes on the flanks of folds in Mesozoic sedimentary rock. These slides generally have volumes of 2×10^4 to 2×10^6 m^3. In areas where the earthquake triggered rock block slides, and throughout this part of the Caucasus, remnants of ancient, similar slides are present.

Debris Avalanches. Several rock and debris avalanches were triggered from steep slopes near the epicenter and in the eastern part of the epicentral area (Fig. 3). Some of these temporarily dammed streams and rivers in the steep terrain. One very large debris avalanche was triggered by the earthquake, and it accounted for 50 of the 114 earthquake fatalities. The earthquake dislodged a mass of Jurassic volcanic rocks about 30×10^6 m^3 in volume from the slopes of the Khokhietis–Tskali River valley above the village of Khokheti (Fig. 3). This rock mass fell about 300 m vertically onto the saturated alluvium of the flood plain at the base of the slope, and much of the surficial alluvium was incorporated into the rapidly moving rock mass. One lobe of the debris avalanche struck and overtopped the 100-m-high ridge that forms the wall of the Khokhietis–Tskali valley. The main mass continued traveling down the valley about 1 km until it reached the larger valley of the Gebura River. The avalanche inundated the Khokhietis–Tskali valley, destroyed the village of Khokheti and its approximately 50 inhabitants, and formed a natural dam 100-m high that impounded a lake 1 to 2 km long. The dam was overtopped and breached within several hours (Borissoff and Rogozhin, 1992).

Unusual Aspects of Earthquake-Induced Landslides

During our brief reconnaissance, we observed some unusual and intriguing landslide processes associated with the Racha earthquake. These include delays of 2 to 3 days between the earthquake and major landslide movement, small co-seismic displacement of active landslides, and somewhat unusual landslide failure geometries. Such phenomena have seldom been documented and, in some cases, challenge current ideas about seismic landslide behavior.

Delayed Landslide Movement

The Racha earthquake triggered movement of two very large and destructive earth slides. In both cases, co-seismic landslide displacement was minute, and major episodes of landslide movement occurred 2 to 3 days after the earthquake.

The Zhashkva Landslide. An earth-slide complex at Zhashkva (Fig. 3) covers about 1.5 km^2 in a broad, bowl-shaped reentrant with 5° to 10° slopes that contains a larger ancient landslide complex in Oligocene–Miocene claystone of the Maikop Formation. The upper margin of the recently active, pre-earthquake slide is broadly arcuate but locally irregular. The slide extends downslope to an incised stream channel. Discrete lobes in the complex converge to the central axis of the bowl. The topography is benched, which indicates that multiple landslide blocks moved semi-independently of one another.

Earthquake-triggered displacement along the main scarp ranges from a few decimeters, where scarp morphology is simple, to about 20 m, where the scarp contains multiple internal scarps, grabens, sag ponds, and extension fractures (Fig. 7). Many fractures near the scarp had standing water only 10 to 20 cm below the ground surface. The main scarp indiscriminately crosses several ridges and deep gullies, which indicates a very deep basal shear surface, perhaps 30 to 60 m.

Much of the surface of the landslide is undisturbed and indicates that some parts of the slide moved as discrete blocks with little or no internal deformation. Other areas are pervasively fractured, both parallel and perpendicular to the direction of movement. Most fractures are extensional, but some form series of uphill-facing scarps whose geometry indicates local forward rotation or toppling of the slide mass. In the central part of the

slide complex, two discrete lobes collided almost at right angles, which caused one lobe to be thrust up into a prominent east–west-trending ridge (Fig. 8). At the point of collision, the ridge is bounded by a steep scarp 2 to 7 m high that exposes nearly horizontal slickensides. Downslope from this scarp is a compressional zone of folding and thrusting. On the lower parts of the slide mass, compressional features are common.

Eyewitnesses stated that only a few small cracks formed near the main scarp during the earthquake and that the landslide did not move for 3 days following the earthquake. The major movement that created the features described above began 3 days after the earthquake and continued for 2 days. Eyewitnesses further stated that little rain fell in the days following the earthquake and that the onset of movement did not correlate with strong aftershocks.

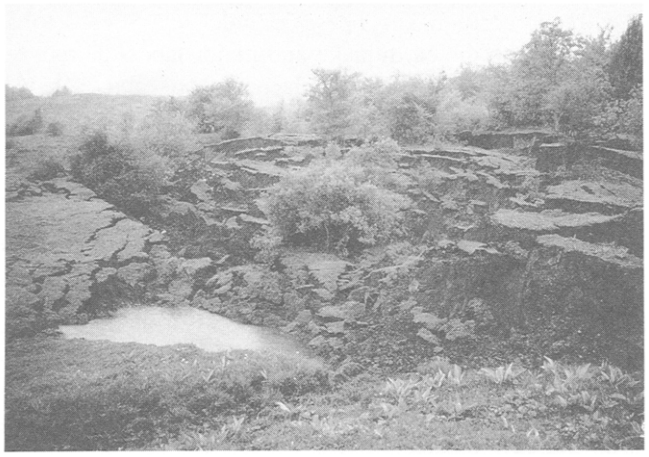

Figure 7. Complex part of main scarp of Zhashkva earth slide; total displacement is about 20 m. Note multiple scarps; deep, filled sag pond; and high degree of disruption of ground surface, all of which formed as a result of the earthquake.

The Chordi Landslide. The second earth slide we investigated destroyed the village of Chordi (Fig. 3). This slide also is a reactivated feature in a valley underlain by claystone of the Maikop Formation. The slide is roughly rectangular in plan and averages about 500 m wide by 1000 m long and is 30 to 50 m deep; thus, the volume is 15 to 25 $\times$ 10^6 m^3 (Fig. 9).

The main scarp that formed as a result of the earthquake has 20 to 30 m of cumulative vertical displacement and several tens of meters of lateral displacement. The weak claystone exposed along the main scarp and the slide margins were sheared extensively by the slide movement, and drainage was diverted along these highly erodible margins. The disaggregation and saturation of this weak material created mud flows along most of the length of the main scarp and along parts of the lateral margins. In some areas, the lateral margins of the slide are defined by vertical scarps as high as 10 m.

The surface of the slide mass shows deformation similar to that of the Zhashkva slide; some areas are relatively intact, but most of the surface is pervasively fractured and folded (Fig. 10). The Chordi slide, however, appeared to have moved more or less as a single slide

Figure 8. Ridge formed by collision of two lobes of the Zhashkva earth slide. One lobe (flat area to the left of the dark-colored scarp) moved from left to right and was thrust beneath the lobe that moved obliquely from the bottom right toward the top left of the photo. The scarp on the left side of the ridge is 7 m high and exposes horizontal slickensides. Note small compressional ridges and thrusts on right side of ridge.

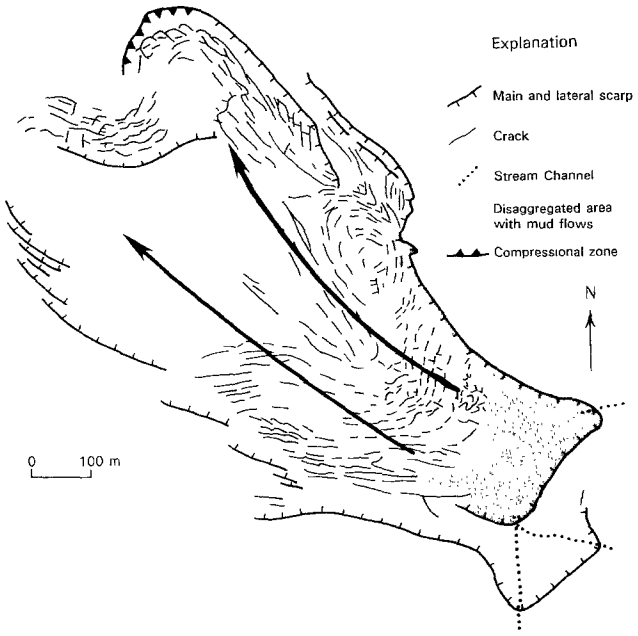

Figure 9. Sketch map of Chordi earth slide. Arrows show direction of landslide movement.

block with small subsidiary slumps, slides, and flows along the margins. Grabens as deep as 10 m and as wide as 20 m formed on the slide mass. The toe of the slide is convex and has been folded in compression. The upper part of the toe has slumped and formed a stepped surface. The medial toe rotated forward and failed by toppling; it forms a very steep, highly fractured and disrupted surface of uphill-facing scarps. The lowest part of the toe is saturated and disaggregated into a mud flow.

Eyewitnesses stated that the Chordi slide was intermittently active before the earthquake. Little or no damage to the single-story wood and stone houses occurred during the earthquake, and only minor slide movement (a few small cracks) was reported. Two or three days after the earthquake, the slide began moving about 8 m/day; this rapid movement caused all the observed damage and destroyed all the structures in the village. At the time of our visit (18 May 1991), the slide was moving about 2 m/day, and the main scarp, slide margins, and toe were actively sliding and enlarging. We estimate the total postearthquake movement of the slide as of 18 May 1991 to be 50 to 70 m, based on offset fences and roads.

Analogous Landslides from Other Earthquakes. The 3-day delay between the earthquake and the major period of movement of the earth slides at Zhashkva and Chordi is difficult to analyze in the absence of detailed geologic and geotechnical data. Such delayed landslide response has been documented in at least four other earthquakes. The 1959 Hebgen Lake, Montana, earthquake (M 7.1) produced the Kirkwood earth flow, whose overall area (270 by 1000 m), shape (rectangular), type of geologic material (soft clay), type of movement (earth flow/slide), and amount of displacement (30 m) are very similar to those of the Chordi slide. The Kirkwood earth flow, which also had moved aseismically prior to the earthquake, began moving at least 5 days after the earthquake and continued to move for at least a month. Hadley (1964) attributed the delayed movement to increased ground-water flow caused by the earthquake and to an increased slope gradient because the upper half of the slide was tectonically elevated relative to the lower half during the quake.

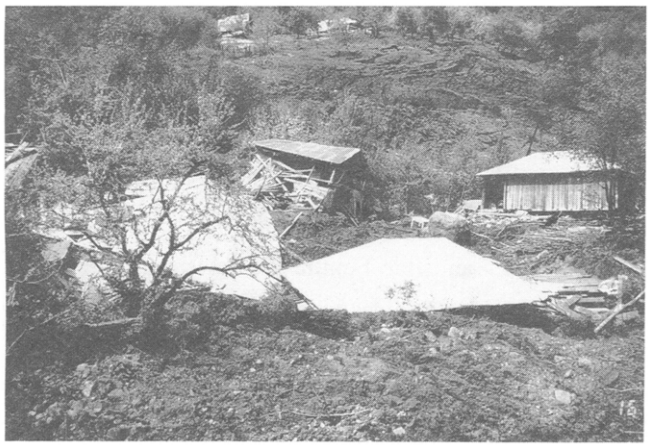

Figure 10. Pervasively fractured and deformed body of the Chordi earth slide. All of the structural damage resulted from landslide movement 3 to 5 days after the earthquake.

The other instances of delayed landslide movement involve debris slides and debris flows. The Cache Creek debris slide (2.5×10^6 m^3) occurred 13 days after the M 8.25, 1906 San Francisco earthquake; Scott (1970, cited in Manson, 1990) surmised that its failure may have been caused by shaking-induced fracturing of the landslide mass and consequent enhanced ground-water percolation. Shaking from the 1949 m_b 7.1 Tacoma earthquake opened cracks several centimeters across on top of a bluff along Tacoma Narrows; 3 days later, a debris slide (0.8×10^6 m^3) occurred there. No cause for the delay has been postulated (Chleborad and Schuster, 1990; U.S. Army Corps of Engineers, 1949). The Lupine Creek debris flow formed 2 days after the 1983 Borah Peak, Idaho, earthquake (M 7.3) and involved 200,000 m^3 of saturated silty sand that flowed more than 3 km down Lupine Creek (Keefer *et al.*, 1985). Keefer *et al.* (1985) attributed the delayed movement to seismically altered hydrologic conditions, postulated by Wood (1985) to involve increased pore pressure due to contractional strain in the hanging-wall block above the normal fault. Hence, this instance is not totally analogous to the Zhashkva and Chordi landslides because they are on the hanging wall above a thrust fault, which is more likely to have dilated in the upper part containing the landslides.

Probable Causes of Delayed Landslide Movement. In these other documented cases, as well as in the Racha earthquake, the simplest explanation for the delayed landslide movement is a change in ground-water conditions. Increased ground-water flow generally results from either increased permeability or increased pore pressure. Wood (1985) stated that increased permeability after an earthquake could result from tectonic fracturing of bedrock near fault zones or from flushing of spring conduits by surging ground-water flows induced by seismic shaking. Observed increases in bedrock permeability following the 1989 Loma Prieta, California, earthquake have been attributed to earthquake-related fracturing of the upper 200 to 300 m of bedrock, which enhanced ground-water flow paths (Rojstaczer and Wolf, 1992). Pore-pressure increases could result from co-seismic contractional strain in the aquifer or from shaking-induced compaction of aquifer rocks (Wood, 1985). In either case—increased permeability or increased pore pressure—a delay of several hours or days to raise ground water in these landslides to critical levels is reasonable for the following two reasons: (1) if the altered hydrologic conditions in the aquifer occurred primarily at depths well below the base of the landslides, then it would take

some time for the increased pore pressure or ground-water flow to migrate upward to the landslides, and (2) the landslide materials are relatively impermeable and would require some time to transmit the increased pore pressures or ground-water flow.

Small Co-seismic Landslide Displacement

The small co-seismic displacements of the active earth slides at Zhashkva and Chordi, as well as many smaller landslides elsewhere, are enigmatic. Many landslides had fresh-looking cracks that initially appeared to have been triggered by the earthquake. Close inspection often revealed vegetation growing in cracks having eroded edges, showing that the observed landslide movement (ranging from a few decimeters to tens of meters) occurred during the weeks prior to the earthquake, probably as a result of spring rainfall. Most of these active landslides also moved as a result of the earthquake, but the co-seismic movement generally amounted to only a few centimeters to a few decimeters.

An example of this is an earth slide on the eastern outskirts of Ambrolauri (Fig. 3). From a distance, this slide appeared to have been triggered by the earthquake. The entire slide mass is pervasively fractured; almost all the cracks are purely extensional and indicate shallow (0.5 to 2 m) sliding of surficial clayey soil parallel to the 17° slope of the ground surface. Close inspection of the slide showed that almost all the visible displacement, totaling several meters, occurred before the earthquake, probably within 1 to 2 months of our visit. A few distinctly younger open fractures were present that presumably formed as a result of the earthquake, but total cumulative displacement on these youngest cracks was only about 5 cm. Thus, the total co-seismic movement of the Ambrolauri slide is 1 to 2 orders of magnitude less than the seasonal movement triggered by rainfall.

Probable Causes of Small Co-seismic Landslide Displacements. The small amount of earthquake-triggered movement of many existing active landslides, particularly earth slides, is puzzling. Many of these slides experienced movement during and after spring rains within days or weeks before the earthquake, and the presence of standing water in deep, open fractures on the landslides some weeks after the earthquake suggests that ground-water levels remained fairly high. Thus, the static factors of safety[1] of these landslides probably were only slightly greater than 1 at the time of the earthquake. The dynamic response of landslides to earthquake shaking commonly is modeled (e.g., Wilson and Keefer, 1983; Jibson and Keefer, 1993) using the sliding-friction-block model developed by Newmark (1965), which treats landslides as rigid-plastic materials. In this modeling approach, the co-seismic displacement of the landslide depends solely on its critical acceleration (the acceleration necessary to overcome frictional resistance and initiate movement), which is a simple function of the static factor of safety. Therefore, according to Newmark's model, if the landslides in the epicentral area had static factors of safety at or near 1, they should have experienced very large displacements during the Racha earthquake. Of course, the stability of these landslides may be highly sensitive to small changes in ground-water levels, but even if the factor of safety at the time of the earthquake had been as high as 1.3, Newmark's method would predict co-seismic displacements (estimated using the model of Jibson and Keefer, 1993) much larger than those observed. The modest response of many such landslides thus indicates that Newmark's method cannot be applied to all types of landslides because some geologic materials cannot be modeled adequately as rigid plastics. These earth slides formed in deeply weathered claystone; this cohesive, highly plastic material probably behaves as a viscoplastic rather than as a rigid-plastic material. Such viscoplastic behavior would effectively dampen the dynamic response.

At least two other phenomena may have contributed to the small co-seismic landslide movements. First, the duration and intensity of the shaking produced by this earthquake may have been lower than normal for earthquakes of this magnitude. Second, the predominant frequency of the strong shaking may have been outside the range that would trigger movement of large landslides. High-frequency strong shaking produces short-wavelength incident seismic waves. If the wavelength of the incident waves is significantly shorter than the dimensions of the landslide mass, the waves may have little overall effect on the movement of the mass because different parts of the landslide will simultaneously experience accelerations in different directions. High-frequency shaking thus tends to produce smaller landslides in brittle materials; lower-frequency shaking is more likely to trigger larger landslides in more ductile materials. This could explain the modest co-seismic displacement of the large earth slides, but not the behavior of smaller slides that moved little during the earthquake.

Unusual Landslide Failure Geometries

Two rock block slides that failed along bedding-plane surfaces developed somewhat unusual failure geometries: they rotated in the horizontal plane rather than simply translating downslope along the basal shear surfaces. The reasons for this differ at the two sites.

The Usholta Landslide. At Usholta (Fig. 3), the earthquake triggered a rock block slide 60-m wide, 40-m long, and 15-m thick. It lies on the 10°-dipping south flank of

[1]Factor of safety is the ratio of resisting forces that tend to inhibit landslide movement to driving forces that tend to cause landslide movement; thus, slopes having a factor of safety greater than 1 are stable, and those having a factor of safety less than 1 should move.

an anticline composed of interbedded Cretaceous limestone and weak, fissile shale that has high plasticity when saturated. As shown in Figure 11, the local slope is oblique to the dip of the bedding, and the slide block rotated outward (counterclockwise) from the slope about a vertical hinge line at its left flank. Near the hinge line, a road is cut by a small fracture about 1-m across; on the right flank, where displacement was greatest, the road is offset more than 20 m. This created a V-shaped gap between the main scarp and the slide block (Fig. 12). The main scarp is nearly vertical and reaches a height of 15 m. Slickensides exposed on the basal shear surface dip 15° and indicate that movement began in the direction of the dip of the slope and then rotated toward the dip direction of the bedrock (Fig. 11). As the slide block moved outward, it began to topple forward and thus contains many extension fractures. Compressional features are present in front of and on the toe of the slide.

The interaction of the local topography with the geologic structure caused the complex rotational movement at Usholta. The initial direction of movement was controlled primarily by topography, but, as the slide block broke free from the original slope, the influence of the geologic structure caused the block, which was sliding on a bedding plane, to rotate toward the direction of bedrock dip (Fig. 11).

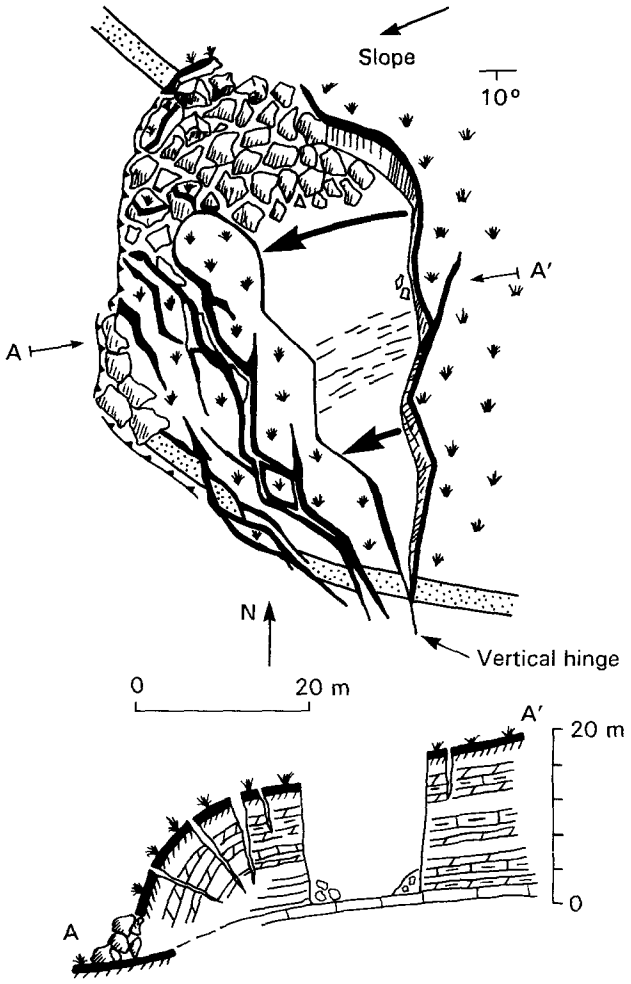

Figure 11. Sketch map and cross section of rock block slide at Usholta. The slide rotated counterclockwise about a vertical hinge line on the right flank of the landslide. Dotted band is offset road.

Shkmeri. The earthquake also triggered a rock block slide on the slope above Shkmeri (Fig. 3); this dip slope also lies on the south flank of the anticline mentioned above at Usholta, where limestone bedrock dips 20° to 40° southward. The slide is about 625 m wide, 150 to 200 m long, and averages about 15 m thick; the volume is thus about 2×10^6 m^3 (Fig. 13). The slide at Shkmeri is similar to that at Usholta in that it rotated outward from the original slope about a vertical hinge line located on the left flank. Thus, displacement is greatest along the right margin and decreases to zero at the left margin (Fig. 14).

The main scarp parallels the slope contour and undulates slightly. The maximum vertical height of the scarp, on the right side of the slide, is about 20 m. Downslope displacement also is greatest—about 50 m—on the right side. Scarp height and landslide displacement decrease toward the left end of the scarp, where the height is only about 1 m and the downslope displacement perhaps 2 m. The left margin is formed by an extension fracture that extends down a preexisting gully, narrows downslope, and ends just above the intersection of the left margin and the toe of the slide; this intersection marks the location of the vertical hinge line about which the slide rotated counterclockwise.

Figure 12. V-shaped gap between the main scarp (left side of photo) and the upper part of the Usholta slide block (right side). Man is standing on the basal shear surface, which dips 15° to the right. Note the decreasing displacement in the direction of view, consistent with rotation about a vertical axis. View is parallel to main scarp.

Figure 13. Rock block slide on slopes above Shkmeri. Landslide block rotated counterclockwise. Scarp on left side of photo has about 50 m of displacement.

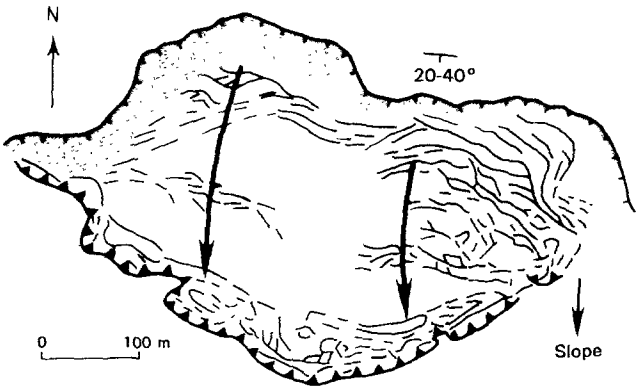

Figure 14. Sketch map of Shkmeri rock block slide. Arrows show direction of landslide movement; other symbols as in Figure 9.

The central part of the slide is broken into several large blocks by fractures as deep as 10 m. Some of the fractures are parallel to the direction of movement and are V-shaped with the open end upslope, which indicates that secondary hinge lines developed within the slide mass as it rotated. Preexisting ridges on the landslide have fractured crests, probably a result of sliding over asperities on the slip surface; compressional deformation during sliding and focusing of strong shaking also may have enhanced ridge-top fracturing. The bottom one-third of the slide mass is a compressional zone containing folds with fractured crests and low-angle thrusts. Compression is greatest on the right side of the toe, where folds have amplitudes of several meters and are severely fractured. Compressional features are smaller toward the left end of the toe, where subtle folds and thrusts have amplitudes less than 1 m.

The surface morphology of the slide mass indicates that the left part of the slide may have moved over an asperity on the basal slip surface. Such an asperity, probably a local variation in bedding attitude, likely impeded downslope movement of the left side of the slide but allowed the right side to slide freely, which caused the entire slide to rotate.

Summary and Conclusion

The M_S 7.0 Racha earthquake of 29 April 1991 occurred on a roughly east–west-striking thrust fault that dips about 20° to 45° north beneath the Great Caucasus Mountains; no surface fault rupture was observed. This earthquake occurred in a continental collision zone that has had only low to moderate historical seismicity. Limited structural damage, a relatively small area affected by landslides, small co-seismic landslide movements, and lack of liquefaction combine to suggest that shaking levels may not have been as great as expected for an earthquake of this magnitude.

Landslides triggered by the strong shaking are abundant over an area of at least 2500 km^2 and caused much of the damage and at least half of the 114 casualties. Rock falls are the most common landslide type triggered by the earthquake, followed (in decreasing order of abundance) by debris slides, earth slides, slumps, rock block slides, and rock avalanches. Local lithology and geologic structure strongly influenced the types and distribution of landslides. The most enigmatic landslide processes associated with the Racha earthquake include (1) time delays of 2 to 3 days between earthquake shaking and landslide movement, most likely caused by changes in ground-water conditions; and (2) small co-seismic displacements of active landslides, probably related to viscoplastic damping of the seismic shaking.

Acknowledgments

The Institute of Physics of the Earth (IPE) of the Russian Academy of Sciences provided logistical support for the American participation in the epicentral investigation. We particularly thank V. Strakhov and J. Aptekman of IPE. John Filson of the U.S. Geological Survey acted as liaison in arranging this joint effort. Ed Harp, Steve Personius, Steve Wesnousky, Dave Keefer, and Bill Cotton reviewed the manuscript.

References

Belousov, T. P. and V. P. Chichagov (1993). Seismic dislocations and the source nature of the Racha, South Great Caucasus, 1991 earthquake, *Trans. Russian Acad. Sci., Phys. Solid Earth* **N3**, 53–63.

Borissoff, B. A. and E. A. Rogozhin (1992). The Racha, Georgia, April 29, 1991 earthquake: results of geological investigation, *Russian Acad. Sci., J. Earthquake Prediction* **1**, 115–125.

Chleborad, A. F. and R. L. Schuster (1990). Ground failure associated with the Puget Sound region earthquakes of April 13, 1949, and April 29, 1965, *U.S. Geol. Surv. Open-File Rept. 90-687*.

DeMets, C., R. G. Gordon, D. F. Argus, and F. Stein (1990). Current plate motions, Geophys. J. Int. **101**, 425–478.

Gorshkov, G. P. (1984). *Regionalnaya Seismotektonika Territorii Yuga SSSR*, Alpiiskii Poyas, Nauka, Moscow (in Russian).

Hadley, J. B. (1964). Landslides and related phenomena accompanying the Hebgen Lake earthquake of August 17, 1959, in *The Hebgen Lake, Montana, Earthquake of August 17, 1959, U.S. Geol. Surv. Profess. Pap. 435*, 107–138.

Jackson, J. (1992). Partitioning of strike-slip and convergent motion between Eurasia and Arabia in eastern Turkey and the Caucasus, *J. Geophys. Res.* **97**, 12471–12479.

Jackson, J. and D. McKenzie (1984). Active tectonics of the Alpine-Himalayan belt between western Turkey and Pakistan, *Geophys. J. R. Astr. Soc.* **77**, 185–264.

Jackson, J. and D. McKenzie (1988). The relationship between plate motions and seismic moment tensors, and the rates of active deformation in the Mediterranean and Middle East, *Geophys. J.* **93**, 45–73.

Jibson, R. W. and D. K. Keefer (1993). Analysis of the seismic origin of landslides: examples from the New Madrid seismic zone, *Geol. Soc. Am. Bull.* **105**, 521–536.

Jibson, R. W. and C. S. Prentice (1991). Ground failure produced by the 29 April 1991 Racha earthquake in Soviet Georgia, *U.S. Geol. Surv. Open-File Rept. 91-392*.

Keefer, D. K. (1984). Landslides caused by earthquakes, *Geol. Soc. Am. Bull.* **95**, 406–421.

Keefer, D. K. and R. C. Wilson (1989). Predicting earthquake-induced landslides, with emphasis on arid and semi-arid environments, in *Landslides in a Semi-arid Environment*, Vol. 2, P. M. Sadler and D. M. Morton (Editors), Inland Geological Society, Riverside, California, 118–149.

Keefer, D. K., R. C. Wilson, E. L. Harp, and E. W. Lips (1985). The Borah Peak, Idaho earthquake of October 28, 1983—landslides, *Earthquake Spectra* **2**, 91–125.

Kondorskaya, N. V. and N. V. Shebalin, Editors (1982). New catalog of strong earthquakes in the USSR, *National Oceanic and Atmospheric Administration, World Data Center A, Report SE-31*, Boulder, Colorado.

Manson, M. W. (1990). Landslide and flood potential along Cache Creek, *Calif. Geol.* **43**, 99–106.

Milanovsky, E. E. and V. E. Khain (1963). *Geology of the Caucasus*, Moscow (in Russian).

Newmark, N. M. (1965). Effects of earthquakes on dams and embankments, *Geotechnique* **15**, 139–159.

Philip, H., A. Cisternas, A. Gvishiani, and A. Gorshkov (1989). The Caucasus: an actual example of the initial stages of continental collision, *Tectonophysics* **161**, 1–21.

Riznichenko, Y. V. and E. A. Dzhibladze (1974). Determination of the maximum possible earthquakes on the basis of comprehensive data on the Caucasus region, *Izv. Earth Phys.* **10**, 317–330.

Rojstaczer, S. and S. Wolf (1992). Permeability changes associated with large earthquakes: an example from Loma Prieta, California, *Geology* **20**, 211–214.

Scott, R. G. (1970). Landslides in Cache Canyon downstream from the Wilson Valley damsites, *Calif. Dept. Water Res., Northern Dist., Memorandum Report (unpublished)*.

U.S. Army Corps of Engineers (1949). *Report on damage resulting from earthquake of 13 April 1949*, Seattle District, Washington.

U.S. Geological Survey (1991). *Preliminary determination of epicenters*, monthly listing, April 1991.

Varnes, D. J. (1978). Slope movement types and processes, in *Landslides—Analysis and Control*, R. L. Schuster and R. J. Krizek (Editors), Nat. Acad. of Sci., Transportation Research Board, Washington, D.C., Spec. Rept. 176, 11–33.

Wilson, R. C. and D. K. Keefer (1983). Dynamic analysis of a slope failure from the 6 August 1979 Coyote Lake, California, earthquake, *Bull. Seism. Soc. Am.* **73**, 863–877.

Wood, S. H. (1985). Regional increase in groundwater discharge after the 1983 Idaho earthquake: coseismic strain release, tectonic and natural hydraulic fracturing, in *Proceedings of Workshop XXVIII on the Borah Peak, Idaho, earthquake*, Vol. A, R. S. Stein and R. C. Bucknam (Editors), *U.S. Geol. Surv. Open-File Rept. 85-290*, 573–592.

Zonenshain, L. P. and X. Le Pichon (1986). Deep basins of the Black Sea and Caspian Sea as remnants of Mesozoic back-arc basins, *Tectonophysics* **123**, 181–211.

U.S. Geological Survey
Denver, Colorado 80225
(R.W.J., C.J.L.)

U.S. Geological Survey
Menlo Park, California 94025
(C.S.P.)

Institute of Physics of the Earth
Academy of Sciences
Moscow, 123810 Russia
(B.A.B., E.A.R.)

Manuscript received 20 April 1992.